Journal of Cardiovascular Computed Tomography (2011) 5, 93–100

Journal of Cardiovascular Computed Tomography

Pictorial Essay

Cardiac CT of non-shunt pathology of the interatrial septum

Carlos A. Rojas, MD[a,*], Camilo E. Jaimes, MD[b], Ahmed H. El-Sherief, MD[a], Hector M. Medina, MD, MPH[a], Jonathan H. Chung, MD[a], Brian Ghoshhajra, MD, MBA[a], Suhny Abbara, MD[a]

[a]*Department of Cardiac Imaging, Massachusetts General Hospital, Harvard Medical School, 165 Cambridge Street, Boston, MA 02114, USA and* [b]*Universidad del Rosario, School of Medicine and Health Sciences, Bogota, Colombia*

KEYWORDS:
Interatrial septum;
Interatrial septal aneurysm;
Lipomatous hypertrophy of the interatrial septum

Abstract. The development and anatomy of the interatrial septum is complex. With the increasing use of cardiac CT and its precise delineation of the anatomy, it is important for the cardiac imager to become familiar with the normal anatomic structures that compose the interatrial septum and their variants. Furthermore, it is important to recognize pathologic processes occurring in this region other than atrial septal defects and potential imaging pitfalls. This pictorial essay provides a detailed review of these topics with emphasis in CT appearance and related technical aspects.

Introduction

Two individual septa, the septum primum and septum secundum, comprise the interatrial septum (IAS). The septum primum arises from the posterior roof of the common atrium, grows toward the endocardial cushions, and eventually fuses with them. Before fusion takes place, small perforations appear in the cephalic portion of the septum primum, which eventually coalesce to create the ostium secundum. The septum secundum is an infolding of the atrial wall that originates in the anterior roof of the common atrium, slightly to the right of the septum primum. This structure grows downward, overlaps the ostium secundum, and forms a tunnel between the 2 atria known as foramen ovale. In approximately 70% of the population, the septum primum and secundum fuse, eliminating this communication (Fig. 1).[1]

Technical aspects of CT imaging of the atrial septum

Cardiac computed tomography (CT) depicts the atrial chambers and the interatrial septal structures in detail with the use of either biphasic or triphasic injection protocols.[2] Biphasic injection protocols consist of an initial contrast phase, followed by a saline injection to clear contrast from the right heart.[3] The strengths of this approach include left heart opacification and shunt detection.[4] Triphasic injection protocols differ by the addition of a middle phase of diluted contrast. The strength of this approach includes better delineation of right-sided cardiac chambers and thus provides a method to image both atrial chambers, in addition to the left-sided structures such as the coronary arteries and left ventricular function.[5]

Conflict of interest: The authors report no conflicts of interest.
* Corresponding author.
E-mail address: caranrojas@gmail.com
Submitted May 29, 2010. Accepted for publication October 18, 2010.

1934-5925/$ - see front matter © 2011 Society of Cardiovascular Computed Tomography. All rights reserved.
doi:10.1016/j.jcct.2010.10.011

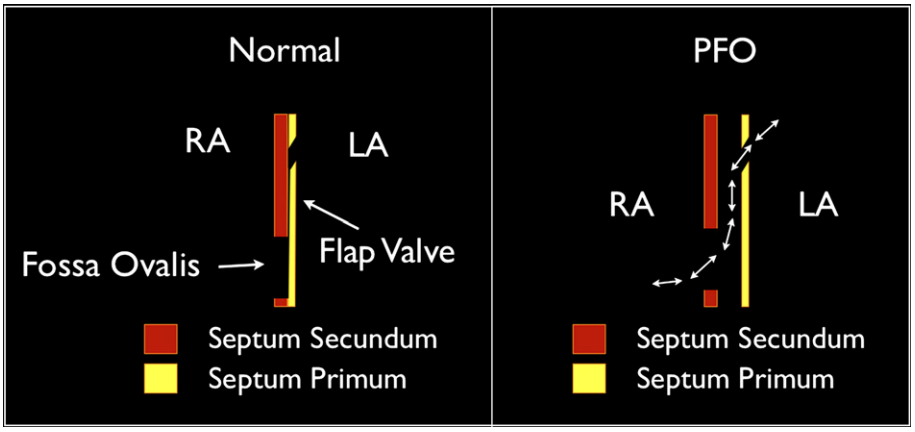

Figure 1 Normal and patent foramen ovale (PFO) appearance of the IAS from a coronal oblique perspective. RA, right atrium; LA, left atrium.

Acquisition of CT data can be gated to the electrocardiogram (ECG) either retrospectively or prospectively. Retrospective gating acquires images through the entire cardiac cycle which allows for image reconstruction at different times in the cycle.[2] Prospective ECG triggering acquires images at a specific time, substantially reducing radiation exposure, but can limit the options for image reconstruction.[6] Following radiation safety policies, prospective gating should be used whenever feasible; nonetheless, if acquisition of images throughout the cardiac cycle yields pertinent information (atrial septal aneurysm, tumors with mobile components), retrospective gating should be favored.

Interatrial septum anatomy and associated structures

The true IAS is defined anatomically and embryologically as the structure between the atria that can be removed without exiting the cavities of the heart. Composed of the flap valve (embryologic remnant of the septum primum) and its bulbous anteroinferior base,[6] the IAS relates to many cardiac structures of main importance. Knowledge of these anatomic relationships is critical because of their clinical, interventional, and surgical implications.

The anterosuperior interatrial groove or septum secundum borders the ascending aorta. A recent CT study reported a mean length of 14.1 ± 4.2 mm.[7] The dimensions of this structure are relevant when considering devices for closure of intravascular atrial septal defects.[8] The anteroinferior rim of the fossa is related to the tricuspid valve, coronary sinus, and Thebesian valve (a thin semilunar fold in the anteroinferior rim of the ostium).[9] Although the valve itself is seldom seen on ECG-gated multidetector CT (MDCT) images, this technique allows for a comprehensive evaluation of the venous anatomy and structures in close proximity (atria and IAS), yielding information useful for endovascular procedures. For example, MDCT can show the presence of a prominent subthebesian pouch or a muscular bridge, which could account for potential complications at the time of canulation.[10]

The triangle of Koch, an important landmark for fast and slow pathways of the atrioventricular node, is closely related with interatrial structures. The inferior vena cava (IVC) valve, also called the eustachian valve, extends from the IVC's ostium to the eustachian ridge. The free border of this valve continues as the tendon of Todaro and serves as the posterior border of the triangle. The anterior border of the triangle is represented by the septal leaflet of the tricuspid valve, whereas the ostium of the coronary sinus and the septal isthmus (ablation target in reentrant tachycardias) make up the inferior border[11] (Fig. 2).

The flap valve is a fibrous remnant of the septum primum that abuts the septum secundum and closes the foramen ovale. In healthy persons it completely occludes the fossa ovalis and prevents intertrial shunting when the left-sided pressure exceeds right-sided pressure. Early in life, mechanical fusion of the septum primum and secundum should take place. When this process fails, a patent foramen ovale (PFO) is present. The principal risk is the development of paradoxical embolism.[6] A recent MDCT study showed a flap valve in 38.3% of patients with a mean length of 9.9 ± 4.4 mm and a mean diameter in the mid-tunnel of 2.6 ± 0.6 mm. A left-to-right shunt was observed in 43.6% of the study participants. Morphologic PFO features associated with shunts include a short tunnel and the presence of an atrial septal aneurysm (ASA). The contrast attenuation of the shunt jet depends on the timing of the contrast injection and the direction of the flow[3] (Fig. 3 and Fig. 4).

The Chiari network is a fenestrated membrane consisting of threads and strands in the right atrium. It extends from the right atrial-IVC junction to the foramen ovale and is thought to preferentially divert blood flow through the foramen ovale during prenatal life. It was first described in 1897 by anatomist Hans Chiari as an embryonic remnant of the right valve of the sinus venosus. With a prevalence of approximately 2%–3% by autopsy and echocardiographic studies, it has been suggested that the presence of a Chiari network may lead to development

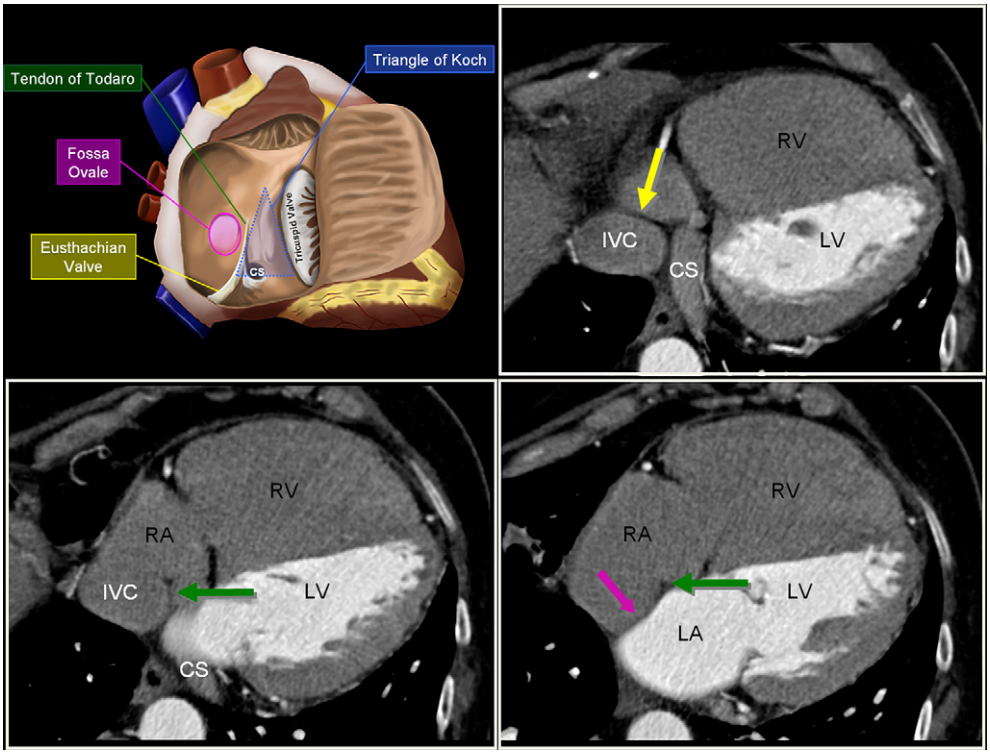

Figure 2 Diagram and axial ECG-gated cardiac MDCT image from a 48-year-old man, showing the eustachian valve (*yellow arrow*), fossa ovalis (*pink arrow*), and the tendon of Todaro (*green arrow*). The triangle of Koch (*blue triangle*) is an important landmark for atrioventricular node fast and slow pathways. CS, coronary sinus; IVC, inferior vena cava; LA, left atrium; LV, left ventricle; RA, right atrium; RV, right ventricle.

of PFOs, ASAs, and episodes of catheter entrapment. Given its association with PFO, patients with Chiari network have an increased incidence of paradoxical embolism. When present, this structure can be seen on echocardiography as a set of "whip-like" mobile threads. CT and magnetic resonance (MR) characterization has not been readily established[12] (Fig. 5).

The Bachmann's bundle (BB) is an interatrial muscular bridge that serves as the main conduction pathway between the 2 atria. On ECG-gated MDCT, BB has a linear structure and follows an oblique course from the right atrial-SVC junction to the base of the left atrial appendage (Fig. 6). A recent study that used ECG-gated MDCT images showed that the BB was visualized less frequently in patients with

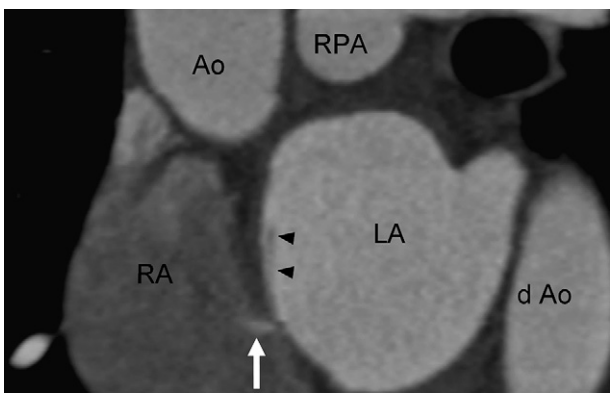

Figure 3 Coronal oblique, ECG-gated cardiac MDCT image from a 60-year-old man with atypical chest pain showing the flap valve of the septum primum (*arrowheads*) as well as a high-attenuation jet extending from a small PFO (*arrow*). This is the typical appearance of a left-to-right PFO shunt. RA, right atrium; RV, right ventricle; LA, left atrium; LVOT, left ventricular outflow tract; Ao, Aorta; RPA, right pulmonary artery; D Ao, descending aorta.

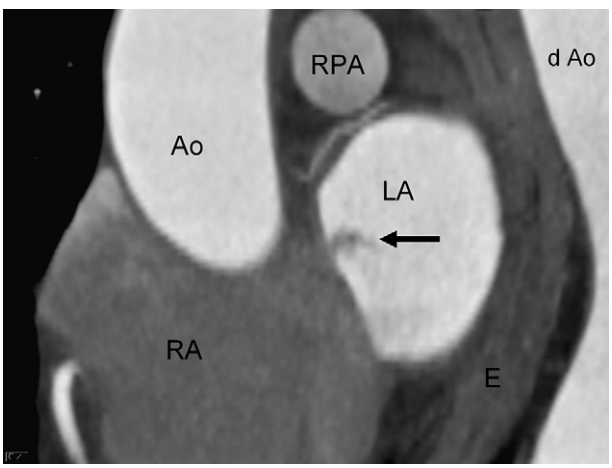

Figure 4 Coronal oblique, ECG-gated cardiac MDCT image from a 38-year-old man showing a low-attenuation jet extending from the PFO to the left atrium because of a right-to-left shunt (*arrow*). RA, right atrium; LA, left atrium; Ao, aorta; d Ao, descending aorta; RPA, right pulmonary artery; E, esophagus.

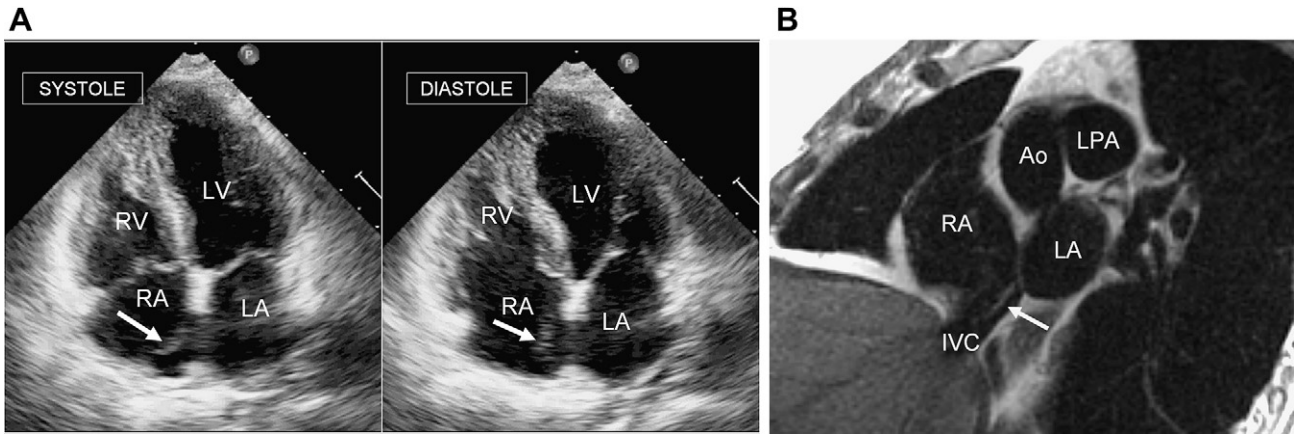

Figure 5 Echocardiographic apical 4-chamber views during systole and diastole (**A**) show a small mobile linear echogenic structure in the right atrium consistent with a Chiari network (*arrow*). Coronal oblique double inversion recovery T1-weighted MR image (**B**) from the same patient shows the Chiari network (*arrow*) as a linear structure, isointense with soft tissue, extending from the IVC-right atrial junction to the interatrial septum. RA, right atrium; LA, left atrium; LV, left ventricle; RV, right ventricle; Ao, aorta; IVC, inferior vena cava; LPA, left pulmonary artery.

interatrial conduction blocks or atrial fibrillation than in healthy controls. This suggests that disease of BB fibers could play a role in the development of atrial arrhythmias.[13]

Interatrial septal pathology

Atrial septal aneurysms

An ASA is defined as an abnormal protrusion of the flap valve with an excursion of $\geq$10 mm beyond the plane of the IAS with a base $>$15 mm.[14] With an autopsy prevalence of approximately 1%,[15] ASA may be an isolated finding or more commonly associated with other structural abnormalities such as a PFO, atrial septal defect, and sinus venosus defect.[14,16]

ASAs can mimic low attenuation lesions arising from the septum such as myxomas in non-gated or bi-phasic prospective imaging, constituting a potential pitfall. The use of a triphasic injection protocol can help assess both sides of the interatrial septum and therefore exclude a space occupying lesion in this region. Retrospectively ECG-gated MDCT images with multiphase reformations can also be helpful in diagnosis by showing the "to-and-fro" motion of the ASA during the cardiac cycle (Fig. 7; Video 1).

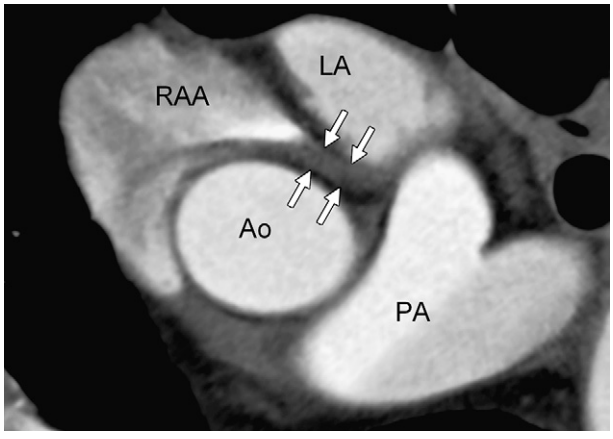

Figure 6 Axial oblique, ECG-gated cardiac MDCT image from a 30-year-old man with atypical chest pain shows a linear soft tissue attenuation structure extending from the superior vena cava-right atrial (SVC-RA) junction to the left atrium consistent with the Bachmann's bundle (*arrows*). RA, right atrium; RAA, right atrium appendage; LA, left atrium; LAA, left atrial appendage; RVOT, right ventricular outflow tract; Ao, aorta; SVC, superior vena cava; PA, pulmonary artery.

Lipomatous hypertrophy of the interatrial septum

Lipomatous hypertrophy of the interatrial septum (LHIAS), first described by Prior in 1964,[17] is defined as an IAS accumulation of adipose tissue exceeding 15 mm and which spares the fossa ovalis. Increased fatty deposits are also found in the subepicardial region, the crista terminalis, the epicardium, and the mediastinum.[18] Its estimated prevalence is 2%–8% by echocardiography and 2.8% by CT.[19,20] LHIAS typically occurs in elderly and obese persons and has been associated with abnormalities in venous drainage,[21] atrial arrhythmias (40% of patients), and sudden cardiac death.[18,22]

LHIAS characteristically appears on CT as a non–enhancing smooth dumbbell-shaped fat density mass that is centered in the IAS and spares the fossa ovale (Fig. 8). MR imaging shows a mass with signal features typical of fat and structural findings identical to those described for CT. Imaging with fluorodeoxyglucose (FDG) positron emission tomography shows increased FDG update from the presence of metabolically active brown adipose tissue in the lesion.[20,23] The differential diagnosis of other fat-containing lesions in this region include lipomas

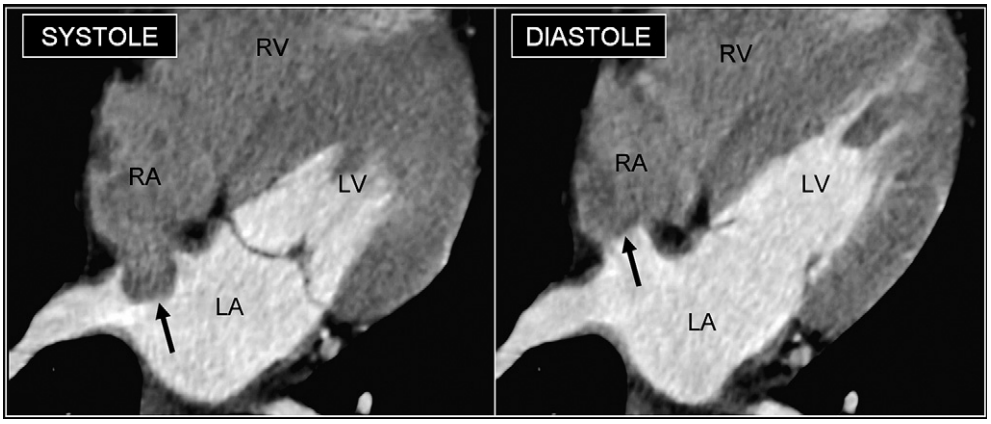

Figure 7 Four-chamber, ECG-gated cardiac MDCT images during systole and diastole show a hypermobile septum of the fossa ovalis with an excursion >10 mm, consistent with an atrial septal aneurysm (*arrow*). Note, that in systole the aneurysm mimics a low-attenuation lesion arising from the septum, such as myxoma. This is a potential pitfall on nongated CT. RA, right atrium; RV, right ventricle; LA, left atrium; LV, left ventricle.

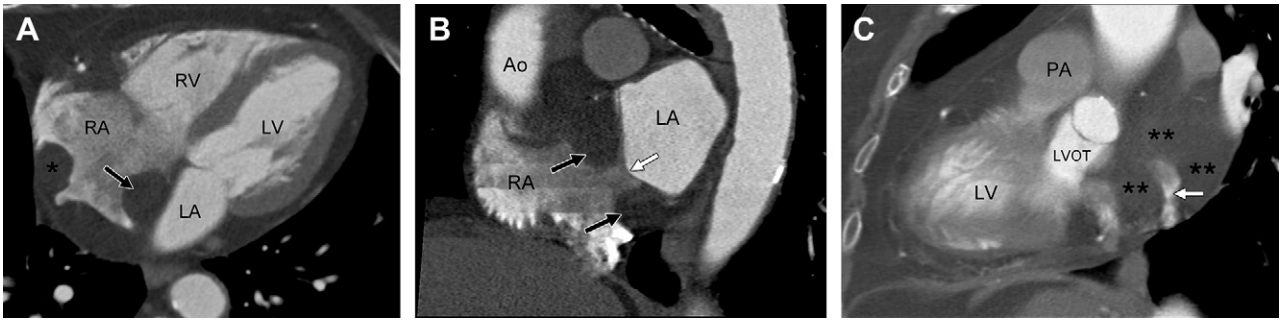

Figure 8 Four-chamber (**A**) and coronal oblique (**B**) ECG-gated cardiac MDCT images show excessive fatty accumulation at the septum secundum with sparing of the fossa ovalis region (*white arrow*) consistent with lipomatous hypertrophy of the IAS (*arrows*). Note additional fatty accumulation of the posterior wall of the right atrium, including the crista terminalis (*asterisk*). Lipomatous hypertrophy of the IAS has been described as a dumbbell-shaped fatty mass as seen Figure 14B. Sagittal oblique ECG-gated cardiac MDCT image (**C**) through the plane of the IAS shows sparing of the fossa ovalis (*white arrow*) with resultant "horseshoe" appearance of fatty accumulation (*double asterisk*). RA, right atrium; RV, right ventricle; LA, left atrium; LV, left ventricle; LVOT, left ventricular outflow tract; Ao, aorta; PA, pulmonary artery.

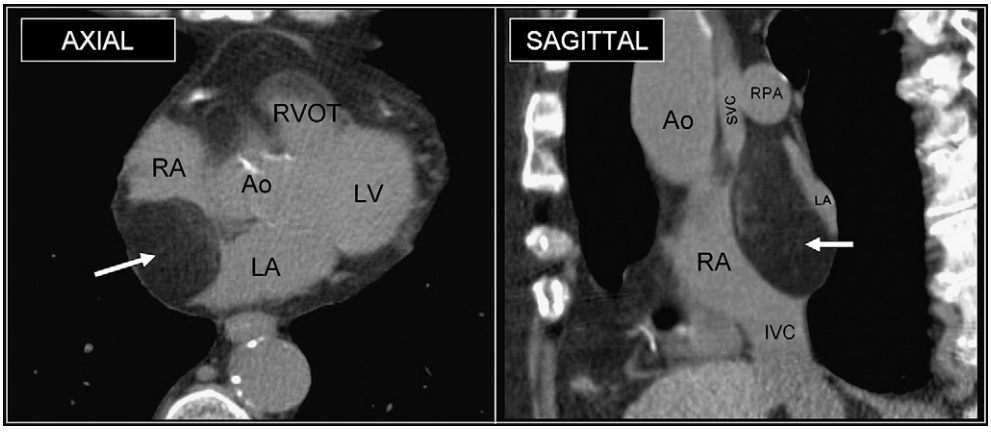

Figure 9 Nongated MDCT images in the axial and sagittal oblique planes from a 65-year-old woman incidentally show a fatty mass in the posterior and superior region of the IAS consistent with an interatrial lipoma (*arrow*). RA, right atrium; RVOTR, right ventricular outflow tract; LA, left atrium; LV, left ventricle; Ao, Aorta; SVC, superior vena cava; RPA, right pulmonary artery.

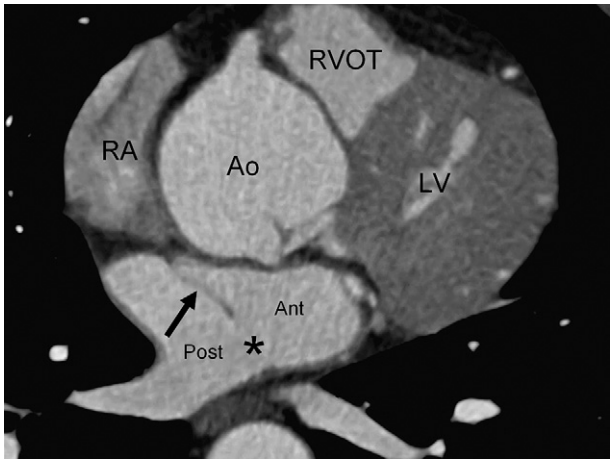

Figure 10 ECG-gated, cardiac MDCT image in axial plane from a 47-year-old man with history of aortic coarctation, ascending aortic aneurysm, and bicuspid aortic valve repair, incidentally show the presence of a septation/membrane (*arrow*) dividing the left atrium into anterior (Ant) and posterior (Post) chamber consistent with cor triatriatum. The patient was clinically asymptomatic because of the presence of a large inferior fenestration (*asterisk*). RA, right atrium; RVOT, right ventricular outflow tract; Ant, anterior left atrium chamber; Post, posterior left atrium chamber; LV, left ventricle; Ao, aorta.

(Fig. 9) and liposarcomas; however, the classic dumbbell appearance of LHIAS is considered pathonogmonic.[23]

Cor triatriatum

Cor triatriatum is a rare congenital anomaly first described by Church in 1868.[24] This uncommon condition accounts for 0.1% of congenital heart diseases and consists of a fibromuscular band that divides the left atrium into 2 chambers.[25] The typical structure of cor triatriatum consists of an abnormal fibromuscular flap arising from the interatrial septum and extending toward the free atrial wall.

Table 1 Common locations for myxomas[27]

Location	Percentage	Specific site within the Atrium	Relative percentage
Left	59	Directly from the fossa ovalis	57
		Free atrial wall	33
		Other	10
Right	28	Directly from the fossa ovalis	63
		Free atrial wall	19
		Other	18
Right ventricle	8	—	—

This septum has a density similar to the IAS and does not enhance, remaining hypodense after contrast injection. The anomalous band divides the left atrium into a posterosuperior chamber (receiving blood from the pulmonary veins) and an anteroinferior chamber (containing the atrial appendage and the mitral valve). This condition has been associated with secundum atrial septal defects, mitral regurgitation, and coronary sinus malformations[25] (Fig. 10).

The prognosis of the condition is poor and is closely related to the degree of obstruction, with 75% of untreated persons dying in infancy because of secondary pulmonary hypertension.[26] Although uncommon, a few cases of adult cor triatriatum have been described, and the presenting symptoms are also the result of long-standing pulmonary venous congestion (dyspnea, orthopnea, and hemoptysis).[25]

Masses

Atrial myxoma

Atrial myxomas are the most common primary neoplasm located in the interatrial septal region and less

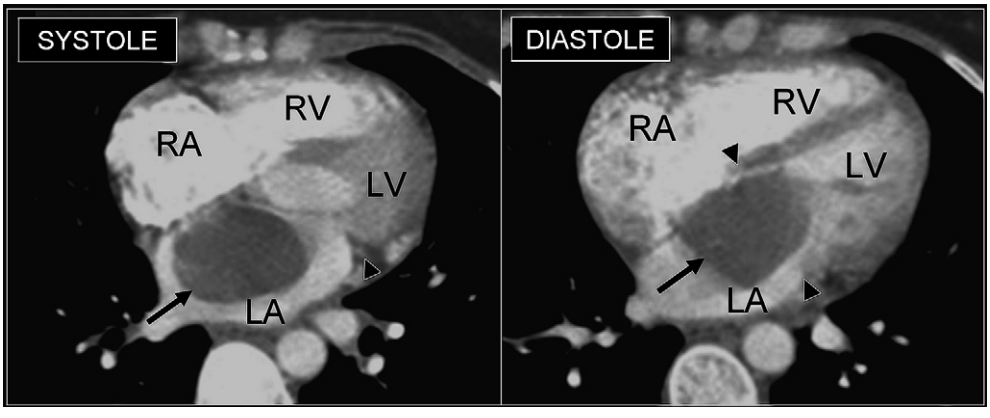

Figure 11 Nongated CT of the chest with contrast in the axial plane from a 37-year-old woman shows a large low attenuation rounded mass in the left atrium attached to the IAS, consistent with a pathology-proven atrial myxoma (*arrow*). Because of the random phase of acquisition on nongated CT, both systolic and diastolic phases of the cardiac cycle are visualized on the same scan and, in this case, allowing the detection of diastolic prolapse of the myxoma through the mitral valve plane (*arrowheads*). RA, right atrium; RV, right ventricle; LA, left atrium; LV, left ventricle.

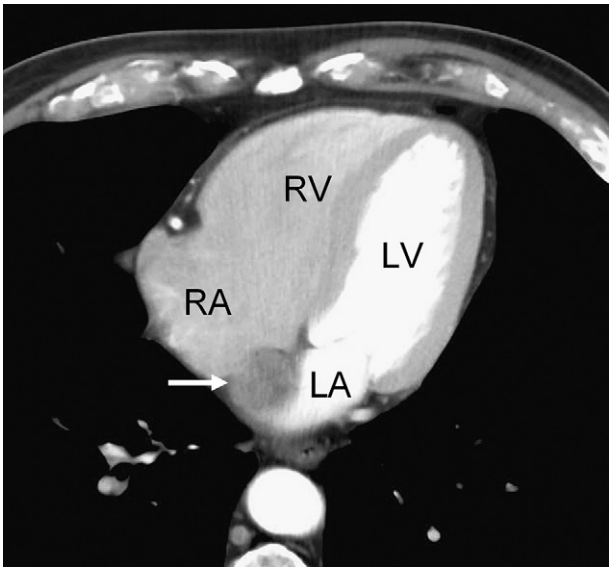

Figure 12 Follow-up, nongated CT of the chest with contrast, in the axial plane from a 75-year-old man with melanoma shows interval development of a heterogenous rounded mass located along the posterior region of the IAS most consistent with a metastatic lesion (*arrow*). RA, right atrium; RV, right ventricle; LA, left atrium; LV, left ventricle.

commonly in other locations (Table 1). Myxomas are most commonly isolated and benign, although 7% of myxomas are associated with Carney's complex, an inherited autosomal dominant disorder characterized by multiple tumors of this kind (mainly in the heart and skin), endocrine hyperactivity, and skin hyperpigmentation.[27] Left atrial myxomas are usually attached to the IAS through a thin stalk, enabling the mass to be mobile. In its most severe presentation, a large myxoma may prolapse through the mitral valve and generate hemodynamic effects that resemble mitral stenosis. Myxoma may also present with constitutional symptoms arising from immune mediators released by the tumor.[27]

Myxomas appear as heterogeneous lobulated masses with low CT attenuation (43 ± 14 HU) usually below that of unopacified blood.[28] Contrast administration is critical because it favors a sharper identification of the mass and its associated stalk, a feature unique to this diagnosis. The typical "to and fro" movement of myxomas can be shown with the use of different imaging methods, providing an additional clue[27] (Fig. 11). MR imaging is also helpful for diagnosing myxomas, which show either isointense or hyperintense T1 signal, heterogeneous T2 signal, and hypointense signal on steady-state free precession gradient echo.[27]

Metastatic tumors

Tumor metastases to the heart are more common than primary cardiac tumors. The most common primary tumors to involve the heart include lung, breast, melanoma, and lymphoma. The highest frequency of cardiac metastases occurs in melanoma,[29] with a bright appearance on T1-weighted images because of paramagnetic metal binding[30] (Fig. 12).

Thrombus and pitfalls

The most common intracardiac mass is a thrombus. Thrombus occurring in the IAS region usually occur in the setting of a predisposing condition such as a chronic indwelling catheter[31] (Fig. 13). The CT attenuation value of thrombus is typically low (approximately 60 HU) and are both noninfiltrating and nonenhancing, including on delayed images.[28]

Mixing of unopacified IVC blood and opacified superior vena cava blood in the right atrium may lead to the false-positive diagnosis of thrombus. In these instances,

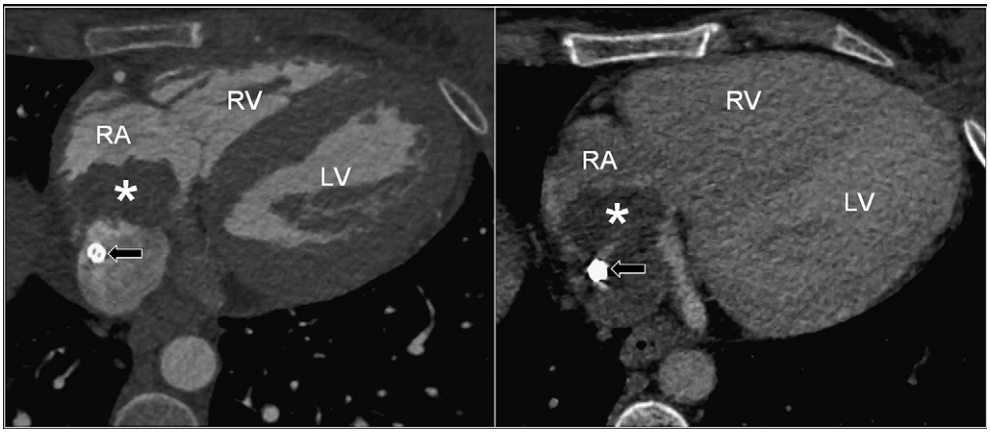

Figure 13 ECG-gated, cardiac MDCT images with arterial (left) and delayed phases (right) show a nonenhancing irregular-shaped filling defect (*asterisk*) in the right atrium (RA) near the IVC-RA junction. This finding resolved on a subsequent echocardiogram after anticoagulation, consistent with a thrombus. Notice the presence of a dialysis catheter (*arrows*). RV, right ventricle; LV, left ventricle.

demonstration of homogeneous opacification in delayed images after contrast excludes the presence of thrombus.

Conclusions

Interpretation of the complex structures of the interatrial region requires a detailed knowledge of septal anatomy, variants, and atrial septal disorders.

Supplementary data

Supplementary material for this article may be found at http://www.CardiacCTjournal.com.

References

1. Anderson RH, Brown NA, Webb S: Development and structure of the atrial septum. Heart. 2002;88:104–10.
2. Taylor CM, Blum A, Abbara S: Patient preparation and scanning techniques. Radiol Clin North Am. 2010;48:675–86.
3. Abbara S, Arbab-Zadeh A, Callister TQ, Desai MY, Mamuya W, Thomson L, Weigold G: SCCT guidelines for performance of coronary computed tomographic angiography: a report of the Society of Cardiovascular Computed Tomography Guidelines Committee. J Cardiovasc Comput Tomogr. 2009;3:190–204.
4. Saremi F, Channual S, Raney A, Gurudevan SV, Narula J, Fowler S, Abolhoda A, Milliken JC: Imaging of patent foramen ovale with 64-section multidetector CT. Radiology. 2008;249:483–92.
5. Hoey ET, Mankad K, Puppala S, Gopalan D, Sivananthan MU: MRI and CT appearances of cardiac tumours in adults. Clin Radiol. 2009; 64:1214–30.
6. Hirai N, Horiguchi J, Fujioka C, Kiguchi M, Yamamoto H, Matsuura N, Kitagawa T, Teragawa H, Kohno N, Ito K: Prospective versus retrospective ECG-gated 64-detector coronary CT angiography: assessment of image quality, stenosis, and radiation dose. Radiology. 2008;248:424–30.
7. Saremi F, Channual S, Krishnan S, Gurudevan SV, Narula J, Abolhoda A: Bachmann Bundle and its arterial supply: imaging with multidetector CT–implications for interatrial conduction abnormalities and arrhythmias. Radiology. 2008;248:447–57.
8. Rajiah P, Kanne JP: Computed tomography of septal defects. J Cardiovasc Comput Tomogr. 2010;4:231–45.
9. Saremi F, Krishnan S: Cardiac conduction system: anatomic landmarks relevant to interventional electrophysiologic techniques demonstrated with 64-detector CT. Radiographics. 2007;27:1539–65. discussion 1566–7.
10. Saremi F, Torrone M, Yashar N: Cardiac conduction system: delineation of anatomic landmarks with multidetector CT. Indian Pacing Electrophysiol J. 2009;9:318–33.
11. Anderson RH, Ho SY, Becker AE: Anatomy of the human atrioventricular junctions revisited. Anat Rec. 2000;260:81–91.
12. Schneider B, Hofmann T, Justen MH, Meinertz T: Chiari's network: normal anatomic variant or risk factor for arterial embolic events? J Am Coll Cardiol. 1995;26:203–10.
13. Saremi F, Channual S, Krishnan S, Gurudevan SV, Narula J, Abolhoda A: Bachmann Bundle and its arterial supply: imaging with multidetector CT–implications for interatrial conduction abnormalities and arrhythmias. Radiology. 2008;248:447–57.
14. Hur J, Kim YJ, Lee HJ, Ha JW, Heo JH, Choi EY, Shim CY, Kim TH, Nam JE, Choe KO, Choi BW: Cardiac computed tomographic angiography for detection of cardiac sources of embolism in stroke patients. Stroke. 2009;40:2073–8.
15. Silver MD, Dorsey JS: Aneurysms of the septum primum in adults. Arch Pathol Lab Med. 1978;102:62–5.
16. Feigenbaum H, Armstrong WF, Thomas R: Feigenbaun's Echocardiography. 6th ed. Philadelphia, PA: Lippincott Williams & Wilkins; 2005:190–1.
17. Prior JT: Lipomatous hypertrophy of cardiac interatrial septum. A lesion resembling hibernoma, lipoblastomatosis and infiltrating lipoma. Arch Pathol. 1964;78:11–5.
18. Heyer CM, Kagel T, Lemburg SP, Bauer TT, Nicolas V: Lipomatous hypertrophy of the interatrial septum: a prospective study of incidence, imaging findings, and clinical symptoms. Chest. 2003;124:2068–73.
19. Wann LS, Sampson C, Liu Y: Cardiac and paracardiac masses: complementary role of echocardiography and magnetic resonance imaging. Echocardiography. 1998;15:139–46.
20. Kuester LB, Fischman AJ, Fan CM, Halpern EF, Aquino SL: Lipomatous hypertrophy of the interatrial septum: prevalence and features on fusion 18F fluorodeoxyglucose positron emission tomography/CT. Chest. 2005;128:3888–93.
21. Kindman LA, Wright A, Tye T, Seale W, Appleton C: Lipomatous hypertrophy of the interatrial septum: characterization by transesophageal and transthoracic echocardiography, magnetic resonance imaging, and computed tomography. J Am Soc Echocardiogr. 1988;1:450–4.
22. Shirani J, Roberts WC: Clinical, electrocardiographic and morphologic features of massive fatty deposits ("lipomatous hypertrophy") in the atrial septum. J Am Coll Cardiol. 1993;22:226–38.
23. Meaney JF, Kazerooni EA, Jamadar DA, Korobkin M: CT appearance of lipomatous hypertrophy of the interatrial septum. AJR Am J Roentgenol. 1997;168:1081–4.
24. Church W: Congenital malformations of the heart: abnormal septum in the left auricle. Trans Pathol Soc Lond. 1868;188–90.
25. Su CS, Lin WW, Lee T, Ting CT, Lian KW: Usefulness of multidetector-row computed tomography in evaluating adult cor triatriatum. Tex Heart Inst J. 2008;35:349–51.
26. Thakrar A, Shapiro MD, Jassal DS, Neilan TG, King ME, Abbara S: Cor triatriatum: the utility of cardiovascular imaging. Can J Cardiol. 2007;23:143–5.
27. Grebenc ML, Rosado-de-Christenson ML, Green CE, Burke AP, Galvin JR: Cardiac myxoma: imaging features in 83 patients. Radiographics. 2002;22:673–89.
28. Scheffel H, Baumueller S, Stolzmann P, Leshka S, Plass A, Alkadhi H, Schertler T: Atrial myxomas and thrombi: comparison of imaging features on CT. AJR Roentgenol. 2009;192:639–45.
29. Roberts WC: Primary and secondary neoplasms of the heart. Am J Cardiol. 1997;80:671–82.
30. Enochs WS, Petherick P, Bogdanova A, Mohr U, Weissleder R: Paramagnetic metal scavenging by melanin: MR imaging. Radiology. 1997;204:417–23.
31. Anavekar NS, Bonnichsen CR, Foley TA, Morris MF, Martinez MW, Williamson EE, Glockner JF, Miller DV, Breen JF, Araoz PA: Computed tomography of cardiac pseudotumors and neoplasms. Radiol Clin North Am. 2010;48:799–816.